Early/fast VLF events produced by electron density changes associated with sprite halos

Robert C. Moore, Christopher P. Barrington-Leigh, Umran S. Inan, and Timothy F. Bell
STAR Laboratory, Stanford University, Stanford, California, USA

Received 12 December 2002; revised 3 June 2003; accepted 22 July 2003; published 14 October 2003.

[1] The magnitudes of scattered fields produced during early/fast very low frequency (VLF) events observed at 13 closely spaced (~65 km) sites are compared with those expected for sprite halo disturbances using a numerical model of wave propagation within the Earth-ionosphere waveguide. Three different early/fast events of varying magnitudes are analyzed using three different nighttime ambient lower ionospheric electron density profiles. The electron density disturbances associated with sprite-halo events are determined using a full-wave electromagnetic (FWEM) model. Observed scattered field amplitudes of typical (VLF amplitude changes of 0.2 dB < ΔA < 0.8 dB) Early/fast events agree with model calculations within a factor of two when the peak return stroke currents (as recorded by the National Lightning Detection Network, referred to in this work as NLDN) are used to determine the sprite-halo characteristics. Scattered field amplitudes associated with larger early/fast events (ΔA > 1 dB) are found to be within a factor of seven for peak currents of causative lightning based on NLDN. However, in previous studies, some sprite-producing lightning flashes have exhibited large slow-tail components, indicating substantial continuing currents and implying charge removal up to 2–3 times larger than that inferred from the peak current reported by NLDN. For the cases discussed in this paper, scattered field calculations using disturbances caused by 2–3 times larger charge removal are found to be within a factor of two of the measured values. VLF scattering from electron density changes associated with sprite halos thus appear to be the underlying cause of at least some of the VLF perturbations observed as early/fast events. *INDEX TERMS:* 2435 Ionosphere: Ionospheric disturbances; 2427 Ionosphere: Ionosphere/atmosphere interactions (0335); 2439 Ionosphere: Ionospheric irregularities; 2487 Ionosphere: Wave propagation (6934); 0669 Electromagnetics: Scattering and diffraction; *KEYWORDS:* lightning, sprite, sprite halo, early/fast VLF events, VLF propagation, lower ionosphere

Citation: Moore, R. C., C. P. Barrington-Leigh, U. S. Inan, and T. F. Bell, Early/fast VLF events produced by electron density changes associated with sprite halos, *J. Geophys. Res.*, *108*(A10), 1363, doi:10.1029/2002JA009816, 2003.

1. Introduction

[2] Early/fast perturbations of subionospheric VLF signals constitute the earliest experimental evidence of direct impulsive coupling of energy released by lightning discharges to the overlying mesosphere and the lower ionosphere [*Armstrong*, 1983]. Observed events occur within 20 ms of the causative lightning flash (i.e., early) and exhibit a rapid onset less than 20 ms in duration (i.e., fast) [*Inan et al.*, 1988]. Although the discovery of early/fast disturbances significantly precedes that of the more spectacular luminous phenomena known as sprites and elves, the physical mechanism responsible for creating the early/fast disturbance is still not quantitatively understood. Previous models have been used to represent the scattering pattern of early/fast disturbances [e.g., *Johnson et al.*, 1999] but have not yet reproduced the absolute magnitudes of the observed VLF signal perturbations. For example, in the case of the sustained heating model proposed by *Inan et al.* [1996b], changes in the amplitude of the subionospheric VLF signal were found to be less than 0.1 dB even under the best circumstances, while typical early/fast event amplitudes lie in the range of 0.2–0.8 dB. Other suggested mechanisms, such as the attribution of the early/fast VLF event to electron density changes caused by elves [*Dowden*, 1996; *Hardman et al.*, 1998], are not consistent with the scattering pattern of observed perturbations [*Inan et al.*, 1996a; *Barrington-Leigh et al.*, 2001].

[3] It has recently been suggested [*Barrington-Leigh et al.*, 2001] that early/fast events may be associated with sprite halos, which result from the intense quasielectrostatic (QE) fields formed above thunderstorms and involve substantial ionization changes at 70–85 km altitudes [*Barrington-Leigh et al.*, 2001]. In this paper we quantitatively assess this possibility, using the conductivity changes determined by a full wave electromagnetic sprite halo model together with recent experimental measurements of early/fast events and

0148-0227/03/2002JA009816$09.00

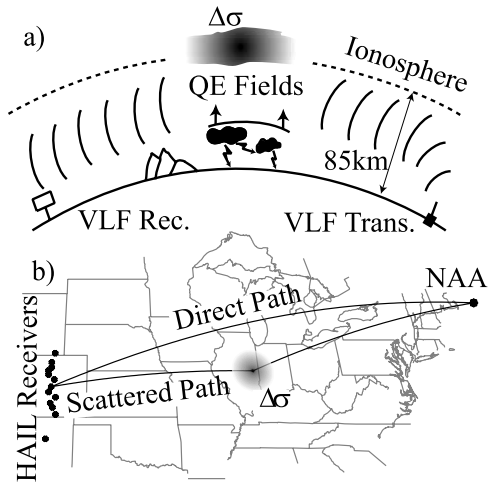

Figure 1. Schematic illustration of a VLF signal being perturbed by the ionospheric disturbance created during an early/fast event.

model calculations of VLF propagation and scattering in the Earth-ionosphere waveguide.

2. Description of the Experiment

[4] VLF data presented in this paper consist of the perturbations of the amplitude and phase of the NAA broadcast signal (24.0 kHz) located in Maine (44.6°N, 67.2°W), as recorded by 13 closely spaced (∼65 km) VLF receivers which constitute the Stanford University Holographic Array for Ionospheric and Lightning research (HAIL) system. A schematic illustration of the NAA-HAIL paths of propagation during an early/fast event is shown in Figure 1. At each receiver, the broadband signal detected by a 1.7 m × 1.7 m magnetic loop antenna oriented to maximize the signal-to-noise ratio of the NAA channel is bandpass filtered to a range of 9–45 kHz and sampled at 10 microsecond intervals, using GPS triggers accurate to within ±0.2 microseconds. The receivers digitally down-convert the individual VLF transmitter signals and record the demodulated amplitude and phase with 20 ms resolution, typically during the time interval 0100 to 1300 UT, when most of the NAA-HAIL propagation paths experience nighttime ionospheric conditions. Typical nighttime noise conditions allow resolutions of 0.1 dB in amplitude and 0.2° in phase for transient events. GPS receivers provide absolute timing accuracy to a greater degree than the data sample rate, thereby providing a stable reference for the phase demodulation.

[5] Data from NLDN is used to determine the time, location, and peak current [*Orville*, 1994] of the lightning discharge(s) associated with each observed early/fast VLF event. Comparison of NLDN-recorded timing of causative flashes with the event onset allows unambiguous identification of an event as the early/fast type as opposed to other types of ionospheric disturbances [*Inan et al.*, 1993], notably those which are caused by lightning-induced electron precipitation from the radiation belts and exhibit typical onset delays of 0.5 to 1.0 s. The intensity of the associated radio atmospherics (sferics in short) in the 25.2 ± 0.15 kHz band recorded at each site provides additional evidence of the time of the causative lightning discharges.

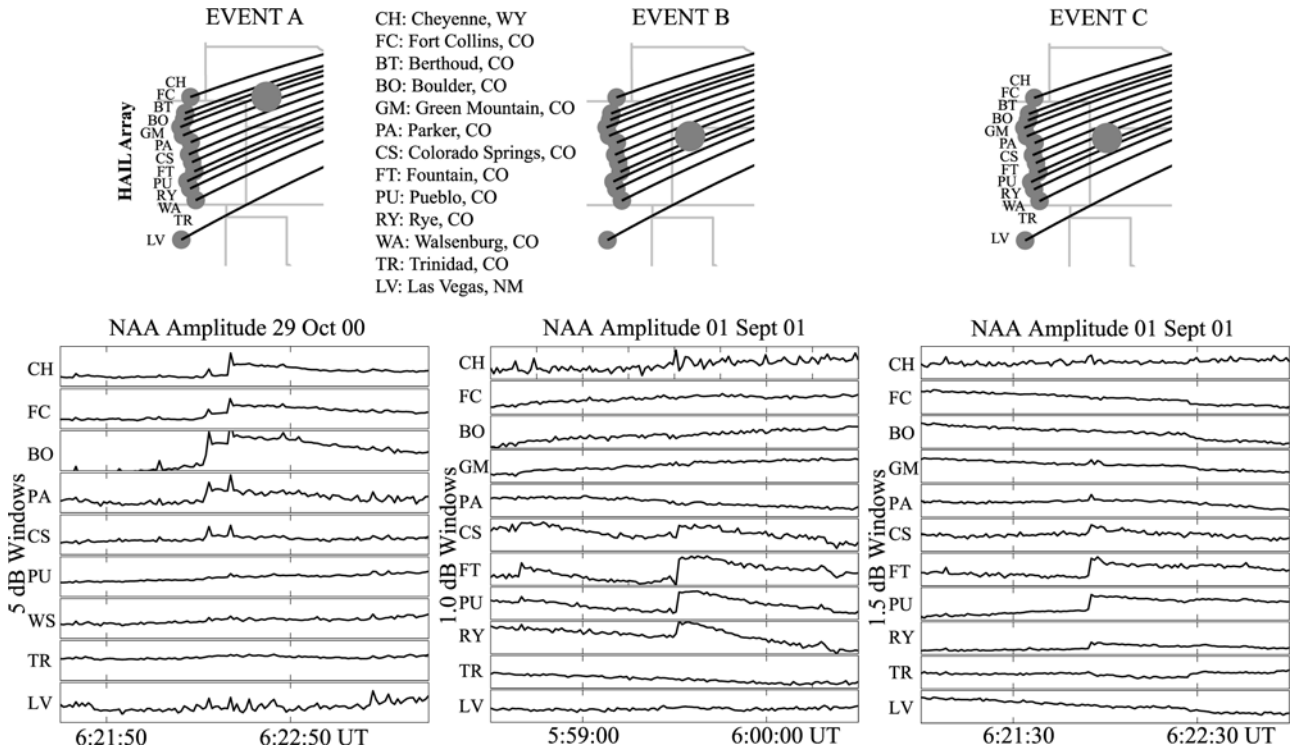

Figure 2. Amplitude traces for three early/fast VLF events measured using the Stanford HAIL receiver array. NAA-HAIL propagation paths are plotted together with the location (provided by NLDN) of the causative lightning strike for each case.

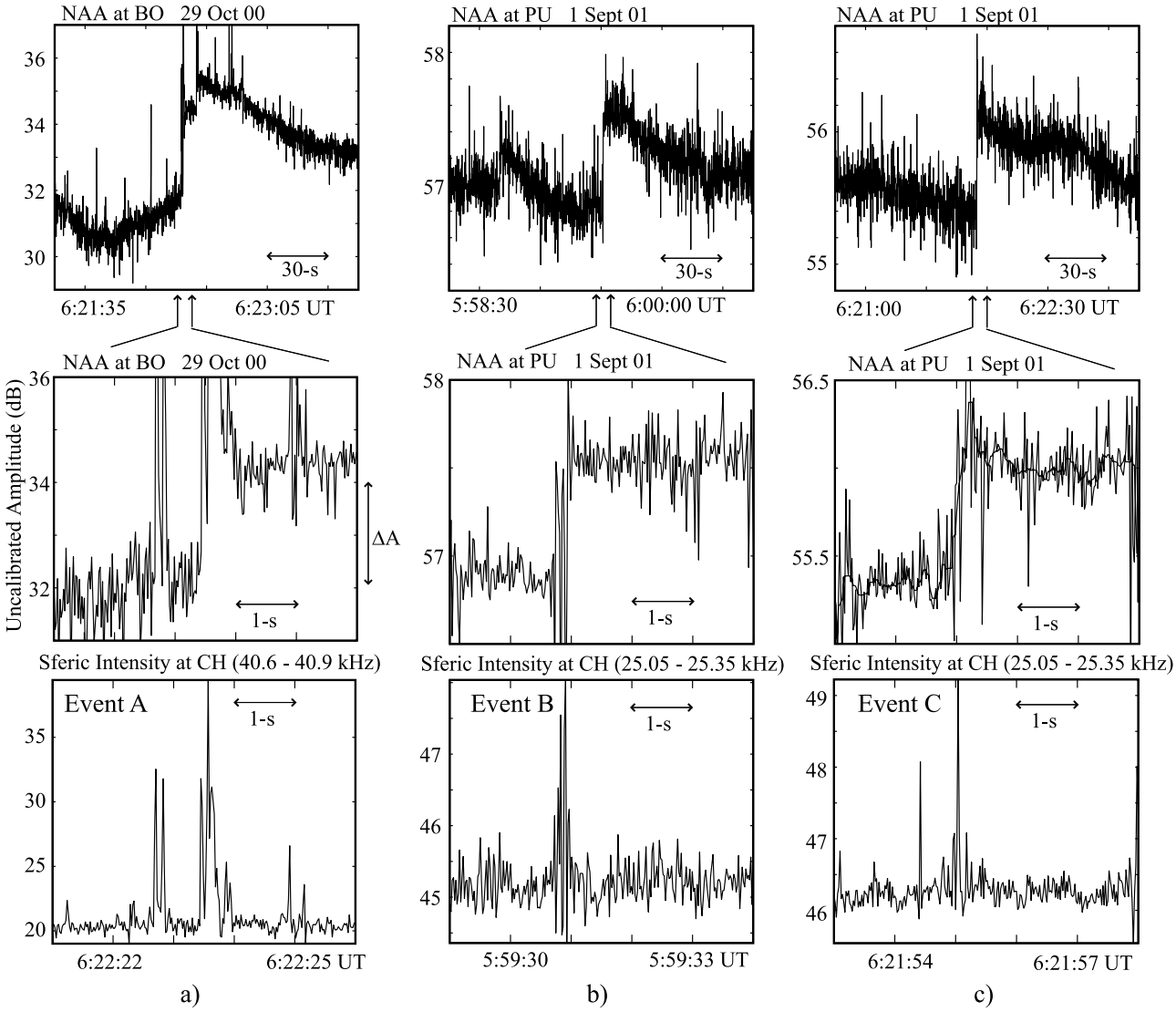

Figure 3. (a), (b), and (c) High-resolution views of the maximum NAA signal perturbation along with the sferic intensity measured in the 25.2 ± 0.15 kHz band for early/fast events A, B, and C, respectively.

[6] Extremely low frequency (ELF) measurements made at Palmer Station, Antarctica, can be used to determine the existence of large continuing currents for the three cases discussed in this paper. However, this data set is currently inconclusive, although it may be explored further in the future. Large continuing currents have been related to positive discharges associated with sprite events, although not exclusively [*Reising et al.*, 1996; *Bell et al.*, 1998]. It has also been shown that sferics with large slow-tail activity have a higher charge moment than would normally be associated with the HF peak currents reported by NLDN [*Reising et al.*, 1996]. Because the discharge duration plays a secondary role to the total charge removed for timescales of 1 to 10 ms [*Pasko et al.*, 1995, 1996; *Boccippio et al.*, 1995], we model a current waveform with a longer duration using a current waveform with a higher peak current. Accordingly, we explore the use of a larger charge moment, represented by the same current waveform and a larger peak current, to model the causative lightning stroke and the associated sprite halo and ionospheric density disturbances.

3. Experimental Data

[7] Three early/fast events, referred to as events A, B, and C, recorded by the HAIL system are considered. Each event is associated with positive cloud-to-ground (CG) lightning strokes as reported by NLDN, although it should be noted that early/fast VLF events are caused by both negative and positive lightning discharges [*Inan et al.*, 1993; 1996c]. Event A was observed in the northern section of the HAIL array as a 2.5 dB perturbation in amplitude and a −17.2 degree perturbation in phase at 0622:23.559 UT on 29 October 2000 in association with a CG discharge of +43 kA NLDN peak current. Figure 2a shows the NLDN reported location of the lightning strike along with the entire HAIL data set for this event. The NAA signal amplitude as recorded at Boulder and the 25.2 ± .15 kHz channel recorded at

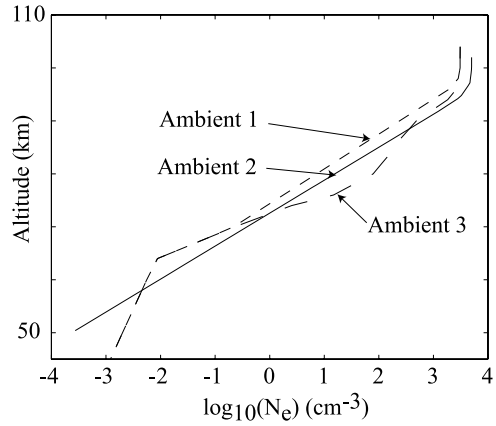

Figure 4. Three nighttime ambient electron density profiles varying from a tenuous (1) to a dense (3) D region.

Cheyenne for this event are shown in Figure 3a. The onset of the event is coincident (within data sampling resolution of 20 ms) with the causative sferic.

[8] Event B was measured as a 0.7 dB perturbation in amplitude and a −1.7 degree perturbation in phase in the middle section of the HAIL array at 0559:30.884 UT on 1 September 2001, and it is associated with a CG discharge of +32 kA NLDN peak current. Figure 2b shows the NLDN reported location of the lightning strike and the entire HAIL data set for this event. The NAA signal amplitude as recorded at Fountain and the sferic intensity in the 25.2 ± 0.15 kHz band recorded at Cheyenne are shown in Figure 3b. Once again, the onset of the early/fast event is coincident (within <20 ms) with the causative sferic.

[9] Event C registered a 0.9 dB perturbation in amplitude and a −0.5 degree perturbation in phase in the middle section of the HAIL array at 0621:55.176 UT on 1 September 2001, in association with a CG having an NLDN peak current of +56 kA. Figure 2c shows the NLDN reported location of the lightning strike and the entire HAIL data set for this event. The NAA signal amplitude as recorded at Fountain and the sferic intensity in the 25.2 ± 0.15 kHz band recorded at Cheyenne are shown in Figure 3c. Once again, the onset of the Early/fast event is coincident (<20 ms) with the causative sferic.

4. Modeling Technique

[10] Three ambient electron density profiles (see Figure 4) are chosen to represent tenuous to dense nighttime D-Region electron densities and also to ensure that modal nulls are not present at the HAIL receiver sites when modeling the 24.0 kHz wave propagation from the NAA transmitter. Such nulls may lead to large amplitude differences for events observed at adjacent HAIL sites and thus complicate the interpretation of the VLF signatures in terms of associated ionospheric density changes. Furthermore, 2-week long quiet-night amplitude averages centered on the date of each of the events studied here indicate that the HAIL sites were not near a signal-null for the cases studied. Ambient profiles 1 and 3 have been used in previous analyses to represent realistic D-region conditions [*Lev-Tov et al.*, 1995; *Inan et al.*, 1992], whereas ambient profile 2 is of the form used by *Wait and Spies* [1964] with $\beta = 0.5$ and $h' = 85$ km. Profile 2 is slightly modified at higher altitudes to be more comparable to the other profiles.

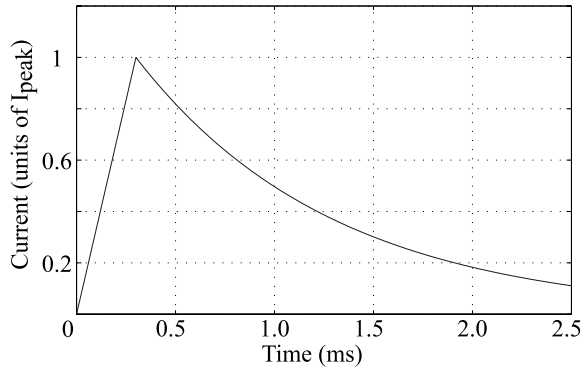

Figure 5. Lightning current waveform used as input to the FWEM model.

[11] Using the chosen profiles, a series of electron density changes were calculated using the cylindrically symmetric full wave electromagnetic model [*Barrington-Leigh et al.*, 2001] of the interaction of the electromagnetic impulses generated by lightning discharges having a channel length of 10 km, exponential decay rates of 1.0 ms, and peak currents of +40 and +100 kA, corresponding to charge moments of 460 C km and 1150 C km. Figure 5 shows the time-dependent current waveform used to model each lightning discharge. The changes in electron density with altitude and radius (as measured from the lightning discharge location) calculated after 1.9573 ms for the 100 kA peak current case and using ambient profile 2 are shown in Figure 6a. The time of 1.9573 ms was used in order to avoid numerical difficulties which occur subsequently in the FWEM calculation and which correspond physically to

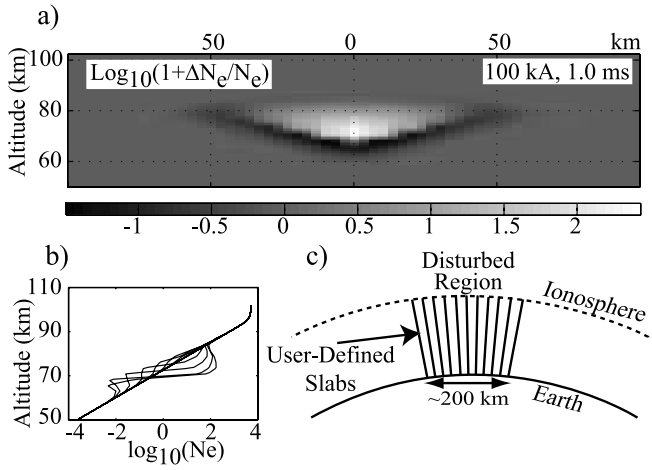

Figure 6. (a) FWEM model simulation of the change in electron density for a sprite halo disturbance caused by a 100 kA peak current, 1.0 ms exponential decay lightning waveform using ambient profile 2. (b) Altitude profiles of the electron densities produced by the simulation in Figure 6a, taken at 10 km intervals in the horizontal plane. (c) Schematic illustration of the LWPC Earth-ionosphere waveguide, including user-defined waveguide slabs in the region of the disturbance.

the spatially irresolvable processes of streamer formation in the center of the disturbed region. We see that resultant electron density changes vary significantly over a lateral distance of one wavelength (12.5 km), suggesting the possibility of strong coupling between waveguide modes when a subionospheric VLF signal is incident on such a disturbance [*Baba and Hayakawa*, 1996].

[12] We wish to determine the absolute amplitude of the scattered fields caused by each of the modeled sprite halo disturbances in order to compare them with experimental data. Based on Figure 6, the sprite halo disturbances involve relatively sharp changes in electron density (both along the propagation direction and as a function of height) so that we expect strong mode coupling to occur within the disturbance region. Unfortunately, we do not have in hand a general enough VLF Earth-ionosphere propagation model which is both three-dimensional (3-D) (so that it can account for the finite transverse extent of the disturbance) and which also accounts for mode coupling within the disturbance. Accordingly, we set out to determine the scattered field amplitudes in an approximate manner, as described below.

[13] The modeling of VLF wave propagation in the Earth-ionosphere waveguide is carried out using the Long Wave Propagation Capability (LWPC) code [*Pappert and Snyder*, 1972; *Pappert and Morfitt*, 1975; *Ferguson and Snyder*, 1987], a multiple-mode model which uses realistic parameters for the ground conductivity, the Earth's magnetic field, and the altitude profile of nighttime ionospheric conductivity. LWPC is a 2-D code which accounts for coupling between waveguide modes and allows for modeling of ionospheric disturbances with user-defined waveguide slabs that have differing altitude profiles of ionospheric conductivity [*Pappert and Snyder*, 1972; *Ferguson and Snyder*, 1987]. The two-dimensional LWPC code is necessarily limited to modeling the effects of localized disturbances which extend to infinity in the transverse direction, appropriate for disturbances which have lateral extents which are large compared to the distance from the disturbance to the receiver site. Figure 6c schematically shows the Earth-ionosphere waveguide with the user-defined slabs included in the disturbed region, the electron densities for each slab being those depicted in Figure 6b.

[14] To estimate the maximum scattered field magnitude, which occurs on the signal path propagating directly through the center of the disturbance, we first use the two-dimensional LWPC model to determine the forward scattered field due to a disturbance of infinite extent in the transverse direction. We then assume that the ratio of the scattering from an actual 3-D disturbance to that from the infinite slab is similar to that which was found by *Poulsen et al.* [1990] for the case of adiabatic scattering with no mode coupling. The maximum scattered field is then determined by calculating the amplitude and phase of the received signal under both ambient and disturbed ionospheric conditions. The magnitude of the scattered field, E_S, can then be calculated as:

$$\left|\frac{E_S}{E_O}\right| = \sqrt{1 + \left|\frac{E}{E_O}\right|^2 - 2\left|\frac{E}{E_O}\right|\cos(\Delta\Phi)}, \tag{1}$$

where E_O is the magnitude of the ambient electric field, E is the magnitude of the electric field under disturbed conditions, and $\Delta\Phi$ is the difference in phase between the two fields. The form of equation (1) shows that it is natural to express the scattered field magnitude normalized by the ambient electric field. Accordingly, scattered field magnitudes quoted in this work are normalized by the ambient electric field in the manner of equation (1). Using the scattered field formulation of *Poulsen et al.* [1990], the ratio of each modal component of the 3-D and 2-D scattered fields has the value

$$\frac{E_{SN}}{E_{S-LWPCN}} = \frac{\alpha a\sqrt{i}}{\sqrt{1 + i\alpha^2 a^2}}, \tag{2}$$

where

$$\alpha = \sqrt{k_O S_O \frac{d}{2x_T x_R}},$$

a is the lateral dimension of the disturbance, S_O is the sine of the eigen-angle for each mode existing in the ambient case, k_O is the wave number in free-space, d is the distance from transmitter to receiver, and x_T and x_R are the distances from the disturbance to the transmitter and receiver, respectively, as defined by *Poulsen et al.* [1990]. Although this ratio is slightly different for each waveguide mode, we found that the ratios for the 10 waveguide modes used in our calculations are well approximated (i.e., to within 0.5%) by a single value. The total scattered field can be expressed as

$$Es = \sum_N E_{SN} = \sum_N E_{S-LWPCN} \frac{\alpha a\sqrt{i}}{\sqrt{1 + i\alpha^2 a^2}}. \tag{3}$$

[15] The lateral dimension, a, can be determined by matching the magnitude of the scattered field caused by the disturbance to that caused by an ''equivalent'' Gaussian disturbance, as used by *Poulsen et al.* [1990]. The electron density of the Gaussian disturbance has the form

$$N_G(h) = N_O(h) + [N_C(h) - N_O(h)]e^{-\left(\frac{r}{a}\right)^2}, \tag{4}$$

where N_O is the ambient electron density, N_C is the electron density at the center of the disturbance, r is the radial distance from the center of the disturbance, and h is the altitude. For the Gaussian disturbance, the change in electron density at each altitude, normalized to the maximum change in electron density at that altitude, as a function of distance along the propagation path is shown in Figure 7a. The electron density profile associated with the center of the disturbance calculated for 100 kA peak current using ambient profile 2 can be seen in Figure 7b, and this profile is simply scaled to generate the other profiles seen in Figure 7c, which are inserted into the Earth-ionosphere waveguide in the slabs delimited in Figure 6c. This process is repeated for each disturbance calculated with the full wave electromagnetic interaction model.

[16] The lateral dimension a can then be estimated by iterating through reasonable values until the received field amplitude for the ''equivalent'' Gaussian disturbance matches that of the actual disturbance. The maximum

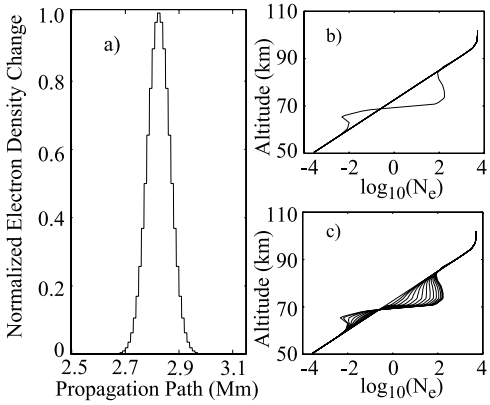

Figure 7. (a) The change in electron density at each altitude, normalized to the maximum change in electron density at that altitude, as a function of distance along the propagation path for the Gaussian disturbance. (b) The ambient and disturbed density profiles used to generate the Gaussian disturbance for the 100 kA peak current, ambient profile 2 case. (c) The Gaussian profiles generated in this manner.

scattered field in the case of the sprite halo disturbance is then calculated using equation (2).

[17] While the above procedure allows us to determine the maximum scattered field amplitude by using the 2-D LWPC code and scaling based on the formulation of *Poulsen et al.* [1990], a 3-D code is needed to determine the actual shape of the scattering (or diffraction) pattern of the sprite halo disturbance and compare it with the data. The scattering pattern, normalized by the maximum scattered field magnitude, can be used to assess the lateral dimension of the scattering disturbance [*Johnson et al.*, 1999].

[18] While a 3-D augmentation of the LWPC code does exist [*Poulsen et al.*, 1993; *Lev-Tov et al.*, 1995], it does not take into account the coupling between waveguide modes within the disturbance region. Coordinates of the disturbance location, along with a radial dependence and conductivity profile, constitute the input parameters to this code. The propagation from the transmitter to the disturbance location, together with the scattering in the direction of the receiver caused by the disturbance, is then calculated, and the propagation for the scattered signal from the disturbance to the receiver provides the modeled scattered field phase and amplitude. The total received field is constructed as a vector sum of this signal and the signal calculated to arrive over the direct propagation from the transmitter to the receiver.

[19] We use this code to determine the scattering pattern, noting that the shape of the pattern is not likely to be significantly affected by the mode coupling. For this purpose, we assume that the sine of the eigen-angles of the waveguide modes vary with radius r in a Gaussian manner, with e-folding distance of a, as given by equation (4).

5. Modeling Results

[20] It can be seen by inspection of Table 1 that the measured scattered field magnitudes are not directly proportional to the NLDN peak current of the lightning waveform, as was previously observed in experimental data by *Johnson et al.* [1999]. Table 2 shows that typical early/fast events (e.g., event B) can be reproduced quite well using the FWEM model, while slightly larger events (e.g., event C) can be reproduced within a factor of two. Events larger than 1 dB (e.g., event A) are larger by a factor of seven from that calculated using the NLDN peak current. However, it is important to note that for a 100 kA peak current, the scattered field amplitude measured for event A is consistent with that predicted by LWPC given the electron density profiles calculated by the FWEM model.

Table 1. Event Statistics

	Event A	Event B	Event C
NLDN Peak Current (kA)	+45	+32	+56
Measured Scattered Field Magnitude	.4798	.0834	.1333

[21] The scattered field magnitudes listed in Table 2 for event B, modeled with ionospheric profile 2, appear to be inconsistent with the rest of the table. However, it is important to note that the VLF signal propagating in the waveguide is constituted by multiple waveguide modes so that the comparison of events observed at different locations with different ionospheric conditions is not straightforward. It is precisely for this reason that we employ the LWPC to quantitatively model each case. For the case of event B, modeled with profile 2, in particular, the disturbed ionosphere related to the +40 kA stroke results in a scattered field mode structure with an interference pattern that is near a local maximum at the end of the propagation path. In contrast, the scattered field modal interference pattern for the +100 kA stroke is not near a local maximum at the end of the propagation path.

[22] Figure 8 shows the scattering pattern calculated by LWPC for two of the events compared against the scattered field measured at each HAIL receiver site. Because the scattering pattern of events B and C are strikingly similar, we have omitted plotting the scattering pattern of event B for brevity. It is readily seen from the plots that with the exception of the 100 kA disturbance calculated for ambient profile 3, any of the scattering patterns reasonably match those measured by the HAIL array. The strong forward scattering, apparent in both the measurements and model calculations, identifies this event as an early/fast event [*Inan et al.*, 1996a, 1996b, 1996c] rather than the wide-angle scattering of rapid onset, rapid decay (RORD) events as defined by *Dowden et al.* [1994].

6. Discussion and Summary

[23] Early/fast VLF events provide evidence of a strong coupling between thunderstorms and the overlying meso-

Table 2. Scattered Field Magnitude Normalized by the Ambient Field for Varying Electron Density Profiles

Ambient Profile	Peak Current, kA	Event A	Event B	Event C
Data		.4798	.0834	.1333
1	+40	.0753	.1003	.1014
2	+40	.0668	.1494	.0713
3	+40	.0143	.0288	.0296
1	+100	.6291	.3155	.2807
2	+100	.2374	.2240	.2332
3	+100	.0426	.0868	.0885

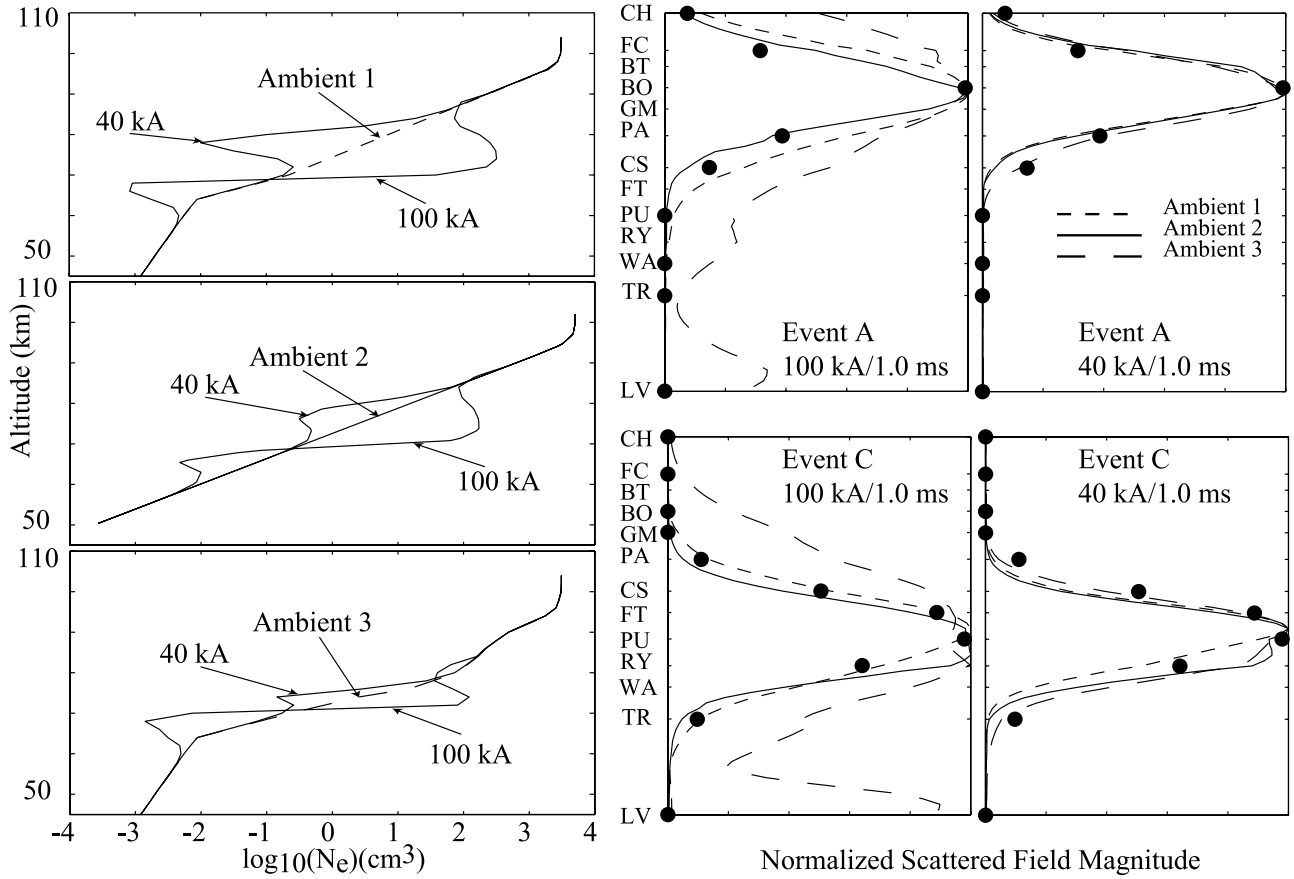

Figure 8. The panels to the left show the altitude profiles for the maximum electron density changes associated with the +40 and +100 kA peak current FWEM simulations for each of the three ambient cases. The panels to the right show the normalized scattered field calculated by LWPC as produced by a Gaussian-shaped disturbance for each case.

sphere/lower ionosphere. These events have been shown to occur frequently [*Sempath et al.*, 2000] and to have a dramatic (6 dB) effect at times [*Inan*, 1993] on the propagating subionospheric VLF signal of interest for time periods ranging from tens to hundreds of seconds for a single event to many hours for the duration of a thunderstorm. The effect of the so-called sprite halo on propagating VLF signals has not yet been fully explored.

[24] In this work, three early/fast VLF events of different magnitudes have been shown to have scattered field magnitudes consistent with those produced by the electron density changes simulated by the FWEM model of a sprite halo disturbance. With one exception, all scattering patterns modeled using the three-dimensional LWPC model are fully consistent with those measured by the HAIL array. The scattered field magnitude of event B, the event with the smallest NAA signal perturbation, was well accounted for by our model using a 40 kA current amplitude, roughly equivalent to the NLDN-measured +32 kA peak current, and 1.0 ms current relaxation timescale in the FWEM calculation. Similarly, the scattered field magnitude of event C, the early/fast event with the next largest NAA signal perturbation, was reproduced to within a factor of 2 using the same model parameters, in spite of the fact that NLDN measured a +56 kA peak current. For these cases, a +100 kA peak current causes a perturbation more than 1.5 times larger than the measured scattered field value in the more tenuous ambient environments. On the other hand, the scattered field magnitude of the largest early/fast event, event A, is reproduced only if we take into account the possibility of large continuing currents during the causative lightning stroke. While the disturbance associated with a +40 kA peak current reproduces within a factor of 7 the measured scattered field magnitude, the disturbance associated with a +100 kA peak current, which is consistent with 2–3 times extra charge removal in the case of large continuing currents, reproduces the measured scattered field magnitude within a factor of 2 and, in fact, overshoots this value by 30% in the more tenuous ambient cases.

[25] Although the aforementioned continuing currents are a likely cause of the discrepancy in the relationship between the charge moments indicated by the NLDN-measured peak currents and the resulting scattered field magnitudes, it is also likely that the modeled perturbed electron density profiles would be more disturbed than the values used in this work if the FWEM calculation could be extended further in time. As mentioned above, this limitation results from the formation of fine spatial structure (sprites) in the disturbed region. The fine structures cannot be resolved by the available model; however, modeled electron density disturbances are generally still increasing with time at the end of the calculation. As a result, the real scattered field

magnitudes resulting from the modeled sprite halos are likely to be larger than the values calculated here and thus to account fully for the observed VLF effect.

[26] Because the FWEM model of the ionospheric disturbance created during the occurrence of a sprite halo has been shown in this work to successfully reproduce both the scattering pattern and the maximum scattered field magnitude of various early/fast events, we conclude that the electron density changes associated with sprite halos are most likely to be responsible for the observed scattering of subionospheric VLF signals during early/fast events.

[27] **Acknowledgments.** This work was supported by the National Science Foundation and the Office of Naval Research under grants ATM-9910532-002 and N00014-94-1-0100-P00006. Participation of C. Barrington-Leigh was supported in part by NASA contract NAS5-98033 at the Space Sciences Lab, University of California, Berkeley. The authors are grateful for the help and support of the many high school teachers and students involved with the HAIL array. We thank K. Cummins and J. Cramer of Global Atmospherics, Inc., for allowing us to use the NLDN data.

[28] Arthur Richmond thanks Steven A. Cummer and another reviewer for their assistance in evaluating this paper.

References

Armstrong, W. C., Recent advances from studies of the Trimpi effect, *Antarct. J. U.S.*, *18*, 281–283, 1983.

Baba, K., and M. Hayakawa, Computational results of the effect of localized ionospheric perturbations on subionospheric VLF propagation, *J. Geophys. Res.*, *101*, 10,985, 1996.

Barrington-Leigh, C. P., U. S. Inan, and M. Stanley, Identification of sprites and elves with intensified video and broadband array photometry, *J. Geophys. Res.*, *106*, 1741, 2001.

Boccippio, D. J., E. R. Williams, S. J. Heckman, W. A. Lyons, I. Baker, and R. Boldi, Sprites, ELF transients and positive ground strokes, *Science*, *269*, 1088, 1995.

Dowden, R. L., Comment on "VLF signatures of ionospheric disturbances associated with sprites" by Inan et al., *Geophys. Res. Lett.*, *23*, 3421, 1996.

Dowden, R. L., C. D. D. Adams, J. B. Brundell, and P. E. Dowden, Rapid onset, rapid decay (RORD), phase and amplitude perturbations of VLF subionospheric transmissions, *J. Atmos. Terr. Phys.*, *56*, 1513, 1994.

Ferguson, J. A., and F. P. Snyder, The segmented waveguide programs for long wavelength propagation calculations, *Tech. Doc. 1071*, Naval Ocean Syst. Cent., San Diego, Calif., 1987.

Hardman, S. F., C. J. Rodger, R. L. Dowden, and J. B. Brundell, Measurements of the VLF scattering pattern of the structured plasma of red sprites, *IEEE Antennas Propag. Mag.*, *40*(2), 29–38, 1998.

Inan, U. S., Lightning-induced disturbances of the lower ionosphere, in *Low-Latitude Ionospheric Physics, Proceedings of COSPAR Colloquium on Low-Latitude Ionospheric Physics, Taipei, Taiwan*, edited by F. S. Kuo, Elsevier Sci., New York, 1993.

Inan, U. S., D. C. Shafer, W. Y. Yip, and R. E. Orville, Subionospheric VLF signatures of nighttime D-region perturbations in the vicinity of lightning discharges, *J. Geophys. Res.*, *93*, 11,455, 1988.

Inan, U. S., J. V. Rodriguez, S. Lev-Tov, and J. Oh, Ionospheric modification with a VLF transmitter, *Geophys. Res. Lett.*, *18*, 705, 1992.

Inan, U. S., J. V. Rodriguez, and V. P. Idone, VLF signatures of lightning-induced heating and ionization of the nighttime D-region, *Geophys. Res. Lett.*, *20*, 2355, 1993.

Inan, U. S., T. F. Bell, and V. P. Pasko, Reply, *Geophys. Res. Lett*, *23*, 3423, 1996a.

Inan, U. S., V. P. Pasko, and T. F. Bell, Sustained heating of the ionosphere above thunderstorms as evidenced in "Early/fast" VLF events, *Geophys. Res. Lett.*, *23*, 1067, 1996b.

Inan, U. S., A. Slingeland, V. P. Pasko, and J. Rodriguez, VLF signatures of mesospheric/lower ionospheric response to lightning discharges, *J. Geophys. Res.*, *101*, 5219, 1996c.

Johnson, M. P., U. S. Inan, S. J. Lev-Tov, and T. F. Bell, Scattering pattern of lightning-induced ionospheric disturbances associated with Early/fast VLF events, *Geophys. Res. Lett.*, *26*, 2363, 1999.

Lev-Tov, S. J., U. S. Inan, and T. F. Bell, Altitude profiles of localized D region density disturbances produced in lightning-induced electron precipitation events, *J. Geophys. Res.*, *100*, 21,375, 1995.

Orville, R. E., Cloud-to-ground lightning discharge characteristics in the contiguous United States: 1989–1991, *J. Geophys. Res.*, *99*, 10,833, 1994.

Pappert, R. A., and D. G. Morfitt, Theoretical and experimental sunrise mode conversion results at VLF, *Radio Sci.*, *5*, 537–546, 1975.

Pappert, R. A., and F. P. Snyder, Some results of a mode-conversion program for VLF, *Radio Sci.*, *7*, 913, 1972.

Pasko, V. P., U. S. Inan, Y. N. Taranenko, and T. F. Bell, Heating, ionization and upward discharges in the mesosphere due to intense quasi-electrostatic thundercloud fields, *Geophys. Res. Lett.*, *22*, 365, 1995.

Pasko, V. P., U. S. Inan, and T. F. Bell, Sprites as luminous columns of ionization produced by quasi-electrostatic thundercloud fields, *Geophys. Res. Lett.*, *23*, 649, 1996.

Poulsen, W. L., T. F. Bell, and U. S. Inan, Three-dimensional modeling of subionospheric VLF propagation in the presence of localized D region perturbations associated with lightning, *J. Geophys. Res.*, *95*, 2355, 1990.

Poulsen, W. L., U. S. Inan, and T. F. Bell, A multiple-mode three-dimensional model of VLF propagation in the Earth-ionosphere waveguide in the presence of localized D region disturbances, *J. Geophys. Res.*, *98*, 1705, 1993.

Reising, S. C., U. S. Inan, and T. F. Bell, Evidence for continuing current in sprite-producing cloud-to-ground lightning, *Geophys. Res. Lett.*, *23*, 3639, 1996.

Sempath, H. T., U. S. Inan, and M. P. Johnson, Recovery signatures and occurrence properties of lightning-associated subionospheric VLF perturbations, *J. Geophys. Res.*, *105*, 183, 2000.

Wait, J. R., and K. P. Spies, Characteristics of the Earth-ionosphere waveguide for VLF radio waves, *Tech. Note 300*, Natl. Bur. of Stand., Boulder, Colo., 1964.

C. P. Barrington-Leigh, T. F. Bell, U. S. Inan, and R. C. Moore, STAR Laboratory, Stanford University, Packard Building, Rm. 355, 350 Serra Mall, Stanford, CA 94305-9515, USA. (cpbl@nova.stanford.edu; bell@nova.stanford.edu; inan@nova.stanford.edu; berto@nova.stanford.edu)